Available online at www.sciencedirect.com
SCIENCE DIRECT®

Journal of Colloid and Interface Science 267 (2003) 456–462

Journal of Colloid and Interface Science

www.elsevier.com/locate/jcis

Unusual wetting dynamics of aqueous surfactant solutions on polymer surfaces

Victoria Dutschk,[a,*] Konstantin G. Sabbatovskiy,[b] Martin Stolz,[c] Karina Grundke,[a] and Victor M. Rudoy[b]

[a] *Institute of Polymer Research eV, Hohe Strasse 6, D-01069 Dresden, Germany*
[b] *Institute of Physical Chemistry of the Russian Academy of Sciences, Leninsky Prospect 31, 119991 Moscow, Russia*
[c] *Sasol Germany GmbH, Paul-Baumann-Strasse 1, 45764 Marl, Germany*

Received 26 December 2002; accepted 15 July 2003

Abstract

Static and dynamic contact angles of aqueous solutions of three surfactants—anionic sodium dodecyl sulfate (SDS), cationic dodecyltrimethylammonium bromide (DTAB), and nonionic pentaethylene glycol monododecyl ether ($C_{12}E_5$)—were measured in the pre- and micellar concentration ranges on polymer surfaces of different surface free energy. The influence of the degree of substrate hydrophobicity, concentration of the solution, and ionic/nonionic character of surfactant on the drop spreading was investigated. Evaporation losses due to relatively low humidity during measurements were taken into account as well. It was shown that, in contrast to the highly hydrophobic surfaces, contact angles for ionic surfactant solutions on the moderately hydrophobic surfaces strongly depend on time. As far as the nonionic surfactant is considered, it spreads well over all the hydrophobic polymer surfaces used. Moreover, the results obtained indicate that spreading (if it occurs) in the long-time regime is controlled not only by the diffusive transport of surfactant to the expanding liquid–vapor interface. Obviously, another process involving adsorption at the expanding solid–liquid interface (near the three-phase contact line), which goes more slowly than diffusion, has to be active.

Keywords: Wetting kinetics; Aqueous surfactant solutions; Polymer surfaces

1. Introduction

Interest in dynamic wetting processes has immensely increased during the past 10 years [1–8]. In many industrial and medical applications, some strategies to control drop spreading on solid surfaces are being developed. One possibility is that a surfactant is added to a liquid [3,8,9].

On the other hand, there are very few systematic investigations of quantitative relations between the chemical structure of surfactants and the spreading behavior of their aqueous solutions on solid polymer surfaces with different surface energies. Moreover, the main part of them is concerned with highly concentrated surfactant solutions (far above the corresponding critical micelle concentrations) [5,10–12]. At the same time, in spite of their practical importance, there is a lack of literature data about the spreading dynamics of relatively dilute aqueous surfactant solutions on polymer surfaces.

The objective of this paper is to present some new results on surfactant solution dynamic behavior observed while measuring the contact angles at different surfactant concentrations both well below and close to the critical micelle concentration (cmc) on different well-prepared and -characterized polymer surfaces. Some problems associated with dynamic contact angle measurements such as evaporation and depletion effects will be also discussed.

2. Materials and methods

2.1. Surfactants

The surfactants used in this study were anionic sodium dodecyl sulfate (SDS), cationic dodecyltrimethylammonium bromide (DTAB), and nonionic pentaethylene glycol mono-

---

* Corresponding author.
E-mail address: vici@ipfdd.de (V. Dutschk).

0021-9797/$ – see front matter © 2003 Elsevier Inc. All rights reserved.
doi:10.1016/S0021-9797(03)00723-9

Table 1
Characteristics of surfactants and their aqueous solutions used in the present study

Surfactant	Molar mass (g/mol)	cmc (g/l)		Surface tension at cmc (mN/m)	
		Reference	Measured	Reference	Measured
SDS	288.4	2.4 [12]	2.4	36.5 [12]	38.3 ± 1
DTAB	308.4	4.5 [13]	4.8	no data found	37.6 ± 1
$C_{12}E_5$	406.6	0.026 [1]	0.031	31.0 [1]	33.0 ± 1

Table 2
Degree of hydrophobicity, film thickness, and surface roughness of polymer samples

Polymer	Water contact angle (°)		Film thickness (nm)	Roughness, RMS (nm)
	Advancing	Receding		(scan area: 20 µm × 20 µm)
Teflon AF	119 ± 1	118 ± 1	40	<2
Parafilm	107 ± 2	106 ± 2	–	42–51
PP	99 ± 4	97 ± 4	20–25	<2
PVF	78 ± 2	67 ± 4	–	120–160
PET	77 ± 2	70 ± 4	–	6–8

dodecyl ether ($C_{12}E_5$), all with the same alkyl chain length. All surfactants were of high purity grade (⩾98%) from Fluka and were used without further purification. Aqueous solutions of these surfactants with desired concentrations in the cmc range of 0.0625 to 2 cmc were prepared by dilution from the corresponding stock solutions with reagent-grade water produced by a Milli-Q filtration system. The cmc values were estimated from surface tension isotherms which were measured by the pendant drop method. Table 1 presents relevant characteristics of the surfactants chosen for wetting measurements.

2.2. Preparation and characterization of polymer substrates

The polymer substrates used in the present study were both polymer foils and spin-coated polymer films. Poly(vinyl fluoride) (PVF) and polyethyleneterephthalate (PET) foils were obtained from Kalle (Wiesbaden, Germany) and Du Pont, respectively. Parafilm M (a paraffin wax surface) is a product of Pechiney Plastic Packaging (USA). The films were prepared using solutions of polypropylene (PP) and Teflon AF on precleaned silicon wafers using a spin coater (SCS, USA). A 6 wt% solution of Teflon AF 1601S (Du Pont) in Fluorinert FC-75 (3M) was diluted with the same solvent in a volume ratio of 1 to 5 to coat the silicon wafers, which were hydrophobized in hexamethyldisilazane vapors for 2 h before the coating. The obtained Teflon AF films were dried at room temperature overnight under vacuum. Finally, to remove residual solvent, the samples were annealed at $T = 165\,^\circ\mathrm{C}$ for 1 h. PP (BASF, Germany) was cast into thin films from a hot 0.5 wt% xylene solution ($T = 130\,^\circ\mathrm{C}$) on the preheated silicon wafers. After casting, the samples were annealed at $T = 50\,^\circ\mathrm{C}$ for 2 h under vacuum.

Sample surface topography was examined using a scanning force microscope Nanoscope IIIa-D3100 (Digital Instruments, USA) in noncontact mode. Film thickness of Teflon AF and PP was determined by a Multiscope Optrel null-ellipsometer (Berlin, Germany) at an incidence angle of 70°.

Advancing and receding contact angles of water drops of volume about 3 to 10 µl were measured by the sessile drop method using a Krüss DSA 10 drop shape analyzer (Germany).

The surface free energies of polymer substrates under investigation, γ_{sv}, were calculated from the experimentally determined advancing contact angles of water using the equation of state for solid–liquid interfacial tension [14],

$$\cos\theta = -1 + 2\sqrt{\gamma_{\mathrm{sv}}/\gamma_{\mathrm{lv}}}\, e^{-0.0001247(\gamma_{\mathrm{lv}}-\gamma_{\mathrm{sv}})^2},$$

where γ_{lv} is water surface tension. The surface free energy values for Teflon AF, Parafilm, and polypropylene are 11.8, 18.4, and 23.2 $\mathrm{mJ/m^2}$, respectively. The surface energy of PVF equals 36.2 $\mathrm{mJ/m^2}$ and it is very close to that of PET (36.7 $\mathrm{mJ/m^2}$).

The roughness data and the film thickness, as well as the water contact angles for all polymer samples, are summarized in Table 2. The small value of the water contact angle hysteresis, e.g., ($\theta_{\mathrm{advancing}} - \theta_{\mathrm{receding}}$), for spin-coated polymer films confirms their homogeneity.

2.3. Wetting measurements and data collection

The wetting measurements were carried out with a FibroDAT 1100 dynamic contact angle tester (Fibro Systems AB, Sweden) equipped with a video camera which collects up to 50 images per second. The device has some advantages over other contact angle measuring systems, which are especially important for performing dynamic wetting measurements with aqueous surfactant solutions: (i) adjustment of specified (small) drop volumes using a liquid delivery system; (ii) tuning of the deposition parameters, such as the distance between a drop and a solid surface, the time difference between drop formation on the syringe tip and drop deposition on the surface, and the intensity of a very short stroke from an electromagnet to release the drop from the tip; (iii) checking the surface tension of surfactant solutions before wetting measurements. A detailed description of this equipment is provided by von Bahr et al. [5] and by Gerdes and Ström [15].

Drops of water or aqueous surfactant solutions of volume about 3 µl were applied to the surface under investigation by a short stroke from an electromagnet. The strength of the stroke was minimized to avoid oscillation effects on the spreading process. The distance between a drop and a polymer surface before its deposition was kept constant (0.6 mm) throughout the series of measurements.

It seems worthwhile to point out that the spreading may be affected by the time difference between drop formation and its deposition. As was shown by Gerdes and Ström [15], the spreading behavior of nonionic surfactant solutions on thiolate-modified gold surfaces depends strongly on the drop lifetime. The drop that was deposited immediately after its formation shows a clear spreading delay. Drops with longer prespreading lifetimes, however, show no spreading delay. In this case, the initially measured contact angles were smaller. In our experiments, drop was deposited on the surface after it was being 15 s equilibrated on the syringe tip.

After deposition, the drop shape was stabilized on the surface after 40–60 ms and reliable data were collected thereafter for at least 30 s.

Our measurements were carried out in the open air at relative humidity of 40 ± 2% and at room temperature of 24 ± 1 °C, which were kept constant.

All polymer surfaces were used for more than one experiment. Between experiments, they were rinsed with Millipore water and pure grade ethanol. To ensure that the surface was not contaminated, the water contact angles were measured after the cleaning procedure. Before contact angle measurements, the equilibrium surface tension of the used solutions was checked using the pendant drop cell integrated into the device.

The FibroDAT gives the drop base radius and the contact angle values from the drop profile. At least 10 separate measurements for each surfactant/polymer system at each solution concentration were used in averaging the dynamic contact angles as function of time. The relative error in the measured initial contact angles (at $t = 60$ ms) calculated as the standard deviation did not exceed 2%. The final (quasi-equilibrium) contact angles were reproducible within 1 to 3%.

3. Results and discussion

3.1. Dynamic and quasi-equilibrium contact angles: evaporation and depletion effects

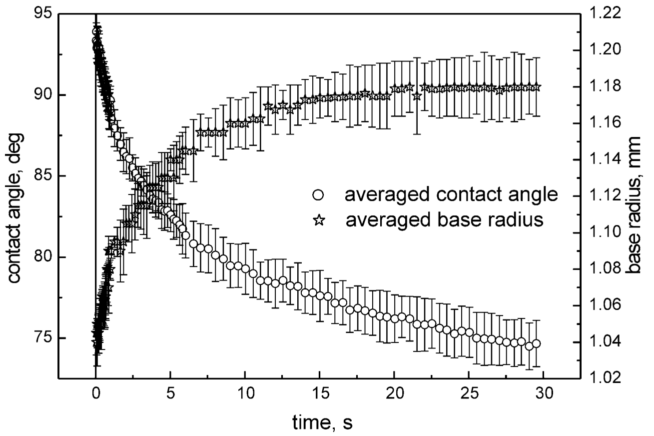

Fig. 1. Averaged contact angle and base drop radius versus time at $C_{12}E_5$ concentration $c = 31$ mg/l (cmc) on highly hydrophobic Teflon AF surface.

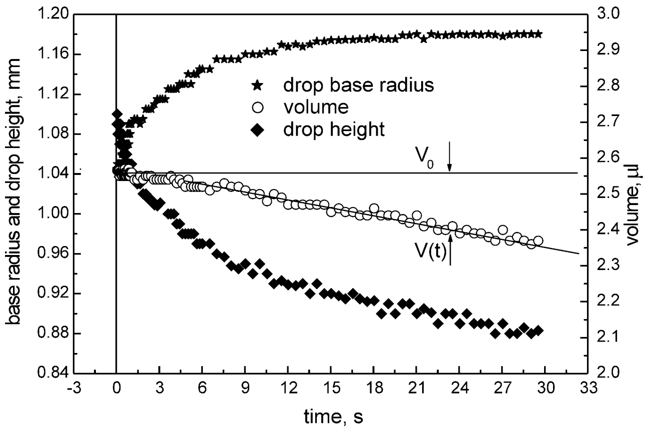

Fig. 2. Measured base radius, height, and volume of a $C_{12}E_5$ drop on Teflon AF surface.

As an example, Fig. 1 demonstrates the averaged dynamic contact angle and drop base radius with their standard deviations for $C_{12}E_5$ solution at the cmc (31 mg/l) on the highly hydrophobic Teflon AF surface. As can be seen, the drop base radius regularly increases and then stays nearly constant, whereas the contact angle does not reach its equilibrium value.

In a typical experiment (Fig. 2), the drop volume decreases linearly with time beginning at approximately 5 s. We proceed from the assumption that the drop volume losses occur due to evaporation caused by relatively low humidity during measurements. Therefore, the drop height decrease can be explained by simultaneous action of two different processes, evaporation and spreading. As a result of evaporation, the measured contact angles may be underestimated (Fig. 3) depending on the radius of the liquid-solid interfacial area [16].

To estimate the "true" contact angle, we followed Starov's suggestion [17] to correct the measured contact angle by assuming volume constancy. In the small-volume limit, the macroscopic shape of the drop is independent of gravity and on a flat surface represents a spherical cap. From simple geometrical considerations [18], the base radius, $r(t)$, for a

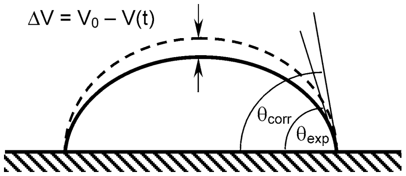

Fig. 3. Schematic of a drop placed on a solid surface; θ_{exp} is the measured contact angle, θ_{corr} is the corrected contact angle, V_0 is the initial volume, and $V(t)$ is the volume that is affected by evaporation.

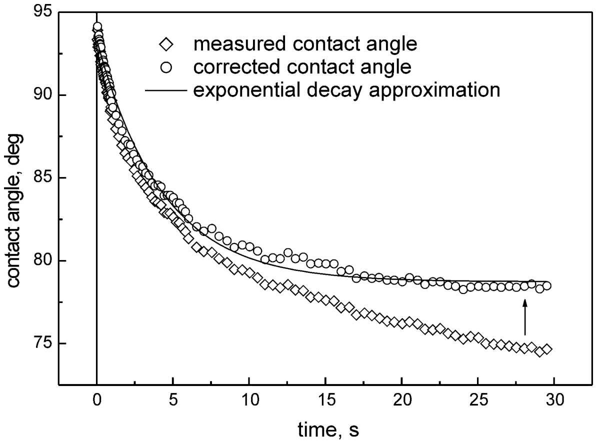

Fig. 4. Measured and corrected contact angles for a $C_{12}E_5$ drop on Teflon AF surface.

small drop can be expressed as

$$r(t)=\left(\frac{6V}{\pi}\right)^{1/3}\frac{1}{\left(\tan\frac{\theta}{2}\left(3+\tan^2\frac{\theta}{2}\right)\right)^{1/3}}, \tag{1}$$

where V is the drop volume, which is assumed to remain constant, and θ is the contact angle, which changes with time. Solving the transcendental Eq. (1) for θ, we obtain

$$\theta(r)=2\arctan\left(\frac{-4+z^{2/3}}{2z^{1/3}}\right), \tag{2}$$

where

$$z=\left(4\frac{6V}{\pi r^3}+4\sqrt{4+\left(\frac{6V}{\pi r^3}\right)^2}\right)^{1/3}.$$

The corrected values of the contact angle were calculated from Eq. (2) using drop radius and the initial volume V_0 data taken from the experiment. All the curves obtained were then fitted by exponential decay function $\theta(t)=\theta_\infty+ae^{-t/b}$ to determine the quasi-equilibrium contact angle θ_∞, which no longer depends on time (Fig. 4). For each surfactant solution/polymer system, the quasi-equilibrium contact angle was obtained as an averaged value from at least 10 experimental radius vs time curves.

In addition to the evaporation effect mentioned above, it should be pointed out that the depletion effect of drop bulk concentration as a result of adsorption at both the liquid–vapor (lv) and solid–liquid (sl) expanding interfaces could be significant for small drops in the case of nonionic aqueous solutions. In fact, to achieve maximum spreading radius for a drop with an initial bulk concentration, c, the following inequality has to be obeyed between the total amount of surfactant, Vc, and the maximal adsorbed amounts, Γ, at both the lv and sl interfaces [5],

$$A_{\text{lv}}\Gamma_{\text{lv}}+A_{\text{sl}}\Gamma_{\text{sl}}\ll Vc,$$

where A_{lv}, A_{sl}, and V represent the equilibrium interfacial areas and the volume of the drop, respectively. In our case, the bulk depletion effect for $C_{12}E_5$ may be manifested for concentrations below $\approx 2\times 10^{-5}$ M, which is of the same order of magnitude as its cmc value ($\approx 6\times 10^{-5}$ M). Thus, this effect may result in overestimation of $C_{12}E_5$ solutions' quasi-equilibrium contact angles. In fact, for the $C_{12}E_5$/Parafilm system, our examination shows that an increase of the drop volume from 3 to 9 µl leads to the decrease of quasi-equilibrium contact angle values by 2°–3° (Table 3). At the same time, the water contact angle for Parafilm does not change with increasing drop volume up to 9 µl.

Table 3
Quasi-equilibrium contact angles for aqueous $C_{12}E_5$ solutions on Parafilm

Concentration (mg/l)	Contact angle (°)	
	$V = 3$ µl	$V = 9$ µl
1.9375	103 ± 1	103 ± 2
3.875	102 ± 2	99 ± 2
7.75	92 ± 1	90 ± 1
15.5	77 ± 1	75 ± 1
31.0 (cmc)	57 ± 1	55 ± 1
46.5	52 ± 1	52 ± 2

For ionic surfactants, the depletion effect does not take place because of their cmc values, which are thousandfold higher than those for nonionic surfactants.

3.2. Spreading behavior of ionic surfactant solutions

Figures 5a and 5b show the curves of solution surface tension and contact angles vs concentration for SDS and DTAB, respectively. Considering the aqueous anionic SDS solutions, we conclude that their surface tension as well as the quasi-equilibrium contact angles for all surfaces studied decrease approximately linearly with increasing surfactant concentration, similar to cationic DTAB solutions, and attain more or less constant values at the critical micelle concentration, as is typical. It can also be seen that the higher the surface energy of polymer substrates, the lower the quasi-equilibrium contact angle. This observation agrees with the well-known results from the literature, for example cf. [19]. However, dynamic wetting behavior of surfactant solutions on solid surfaces, which are different in their chemical nature, has been less investigated and, as consequence, it is less understood.

For highly hydrophobic surfaces, Teflon AF, Parafilm, and PP, the contact angles for DTAB and SDS solutions do not change with time at any concentrations investigated. Our findings agree with the results of Stoebe et al. [6] considering the spreading of aqueous surfactant solutions. They reported

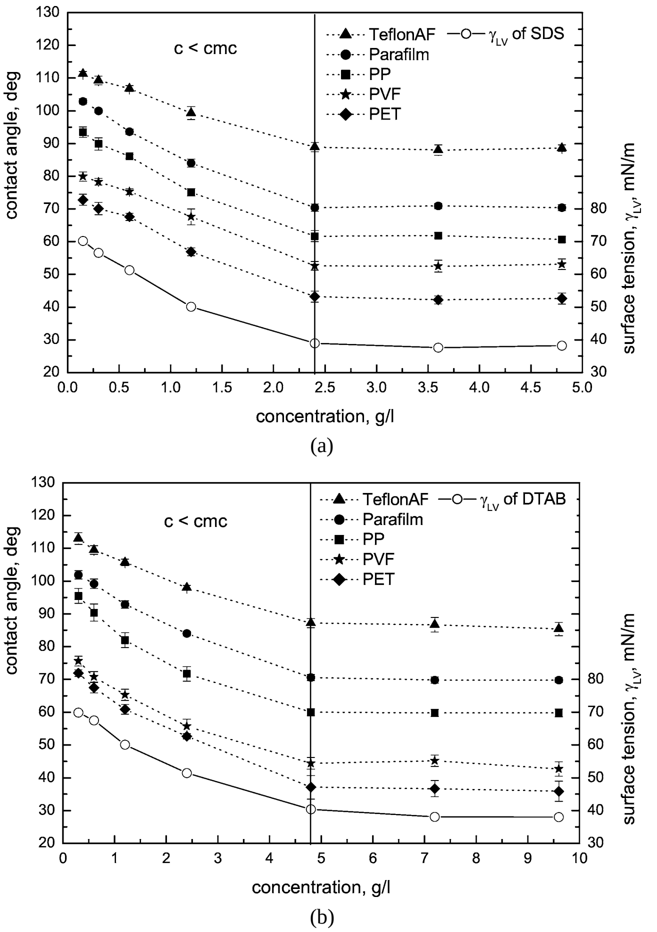

(a)

(b)

Fig. 5. Relationship between the quasi-equilibrium contact angle as well as the surface tension, γ_{lv}, and surfactant concentration for (a) SDS and (b) DTAB for polymer surfaces with different surface energy.

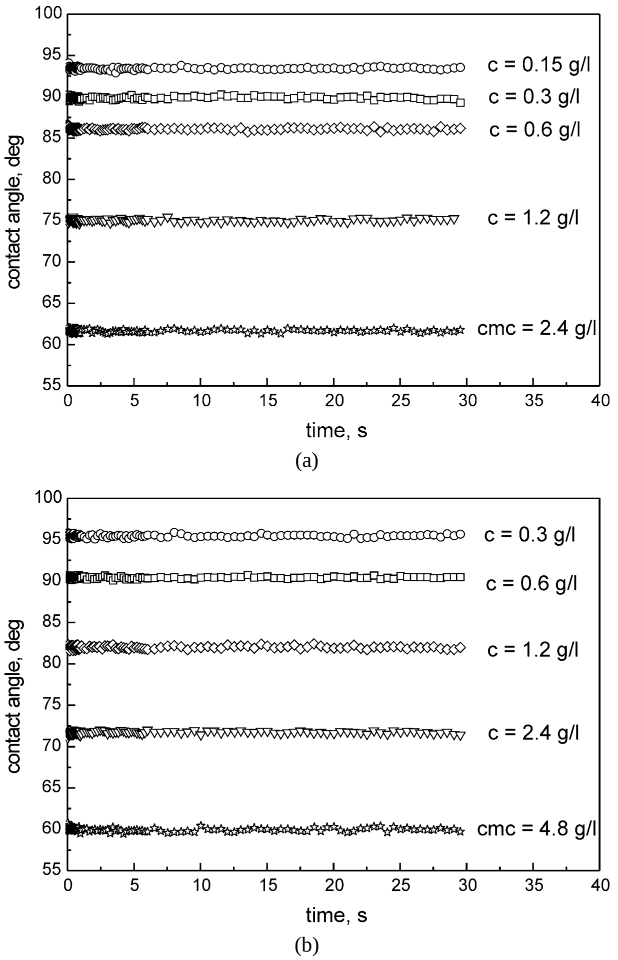

(a)

(b)

Fig. 6. Dynamic contact angles for (a) SDS and (b) DTAB solutions within the whole concentration region on highly hydrophobic PP surface.

that ionic surfactants such as cationic DTAB and anionic SDS do not enhance the spreading of water drops, at least on hydrophobic surfaces. The examples of the wetting behavior of SDS and DTAB solutions on hydrophobic PP surface are shown in Figs. 6a and 6b, respectively. At each concentration, the contact angle presented is the average obtained from analysis of at least 10 experimental curves, which were corrected taking the evaporation effect into account.

In contrast to the hydrophobic surfaces, the contact angles for drops of both ionic surfactant solutions on the moderately hydrophobic surfaces, PVF and PET, strongly depend on time. Figures 7a and 7b show the dynamic contact angles for ionic surfactant solutions on the PET surface. The best fitting for contact angle vs time experimental curves is the exponential decay function, as mentioned above. The fit curves with correlation coefficients $\geqslant 0.9$ are also plotted on the figures.

3.3. Spreading behavior of nonionic surfactant solutions

In contrast to the both ionic surfactants, the contact angle for $C_{12}E_5$ solutions alter with concentration above the cmc, although their equilibrium surface tension does not significantly alter within this concentration region (Fig. 8). The deviation of the contact angle from the surface tension curve is more significant for the more polar solid surfaces, PET and PVF, than for highly hydrophobic Teflon AF and Parafilm. This can be explained by the different structure of the adsorbed surfactant layer near and above the cmc resulting from its rearrangement at $c >$ cmc.

Similarly to the behavior observed for ionic surfactants, nonionic surfactant solutions under investigation spread well over moderately hydrophobic surfaces. Surprisingly, a similar behavior was observed for $C_{12}E_5$ in the case of highly hydrophobic surfaces, but the effect is less pronounced. By way of example, Figs. 9a and 9b demonstrate the dynamic contact angle for $C_{12}E_5$ on Parafilm and PET, respectively.

For highly dilute surfactant solutions, the contact angle on both more hydrophobic and less hydrophobic surfaces does not alter with time. This can be attributed to the absence of adsorption at the solid–liquid interface as a result of the depletion effect mentioned above. Beginning with concentration $c = (1/4)$cmc, our investigations indicate marked dynamic behavior of $C_{12}E_5$ solutions on hydrophobic polymer surfaces, practically independent of the surface energy.

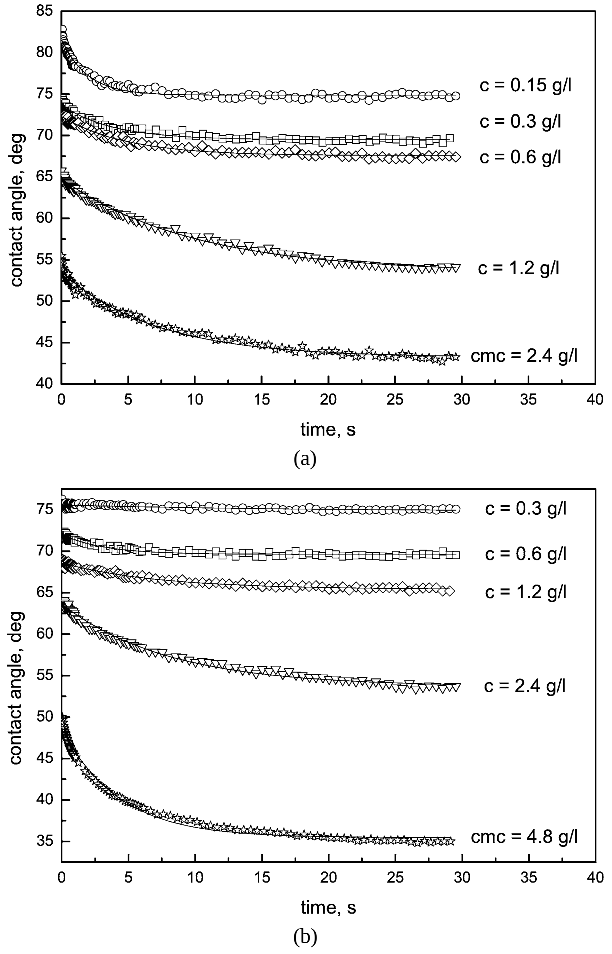

(a)

(b)

Fig. 7. Dynamic contact angles for (a) SDS and (b) DTAB solutions within the whole concentration region on moderately hydrophobic PET surface.

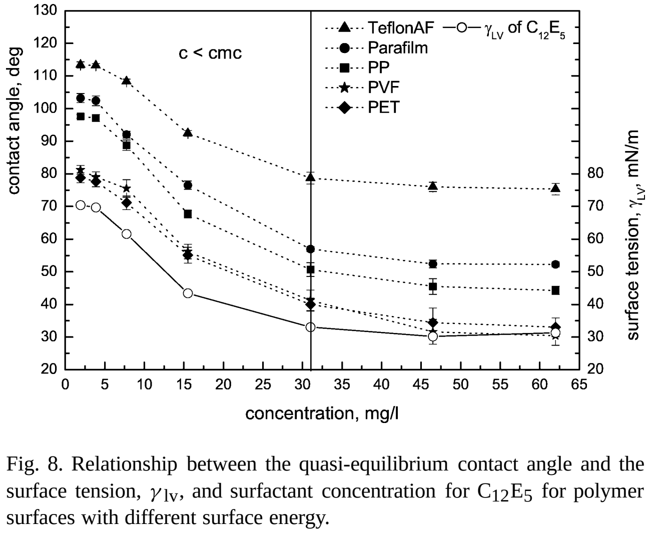

Fig. 8. Relationship between the quasi-equilibrium contact angle and the surface tension, γ_{lv}, and surfactant concentration for $C_{12}E_5$ for polymer surfaces with different surface energy.

The equipment used in this study did not allow measurements of low contact angles, so only the first part of the spreading curve for PET and PVF at concentrations above the cmc was accessible for analysis.

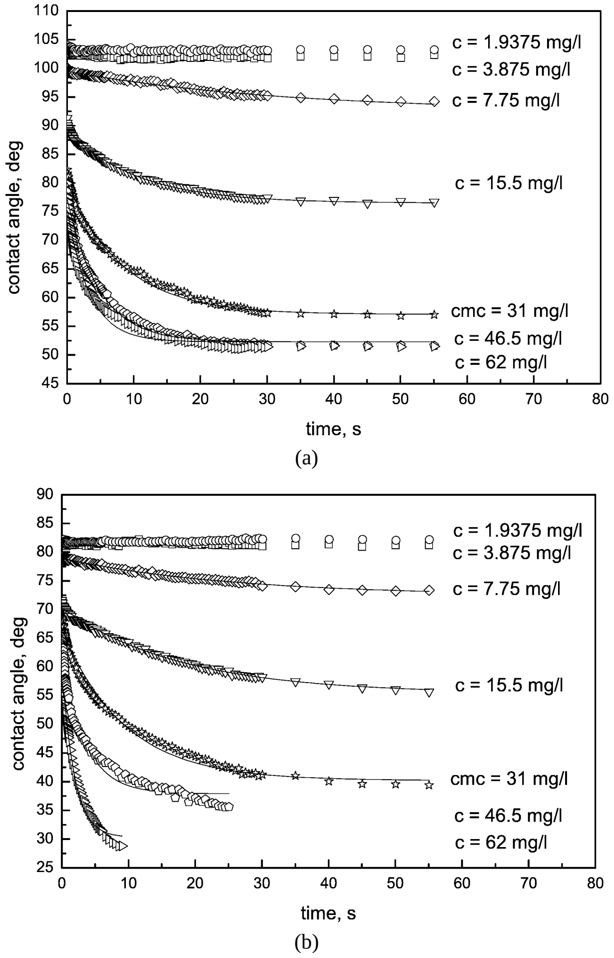

(a)

(b)

Fig. 9. Dynamic contact angles for $C_{12}E_5$ solutions within the whole concentration region (a) on highly hydrophobic Parafilm surface and (b) on moderately hydrophobic PET surface.

Obviously, the adsorption mechanisms should be similar for highly hydrophobic and moderately hydrophobic surfaces within concentration range up to the cmc. Hence, our results confirms the statement of Stoebe et al. [6] that nonionic surfactants exhibited rather universal spreading behavior, which they termed “surfactant-enhanced spreading.”

In general, our results indicate that spreading of both ionic and nonionic surfactants, if it occurs, may be divided into two regimes: the short time regime (fast spreading) and the long time regime (slow spreading). In the first regime, until approximately 1 s, the base radius depends linearly on time. In the second regime, from 1 s to the equilibrium state, the radius values can be fitted by a power function. Exponent values of this power function are lower than 0.1 which disagrees with the concept of the diffusion-controlled spreading according to the idea of von Bahr and co-workers [5]. In their work, a close to linear increase of the drop radius with the square root of time was observed for nonionic $C_{14}E_6$ and $C_{10}E_6$ on thiolate-modified gold surfaces with different hydrophobicity (water contact angle of 22° to 108°). In another work [10], the authors explained this long-time regime in terms of the adsorption process from the bulk to the expanding liquid–vapor interface and the associated surface tension relaxation.

We emphasize that in our case the spreading process goes more slowly than that observed by von Bahr and co-workers. So, we conclude that the spreading is controlled not only by the diffusive transport of surfactant to the expanding liquid–vapor interface. Obviously, another process involving the adsorption at the expanding solid-liquid interface (near the three-phase contact line) should be active which goes more slowly than diffusion. A reasonable explanation for such unusual behavior was given by Starov and co-workers [18]. They described the spreading mechanism of aqueous surfactant solutions over hydrophobic surfaces as a transfer of surfactant molecules on the bare hydrophobic surfaces in front of the moving liquid on the three-phase contact line. The surfactant molecules increase the solid–vapor interfacial tension and hydrophilize the initially hydrophobic solid substrate in front of the spreading drop. This process causes the spreading. Since our measurements, in contrast to the Starov and co-workers measurements, were carried out at relatively low humidity (40%), it is reasonable to assume that hydrophobic surfaces under study were really “dry” in this case. Therefore, the absence of adsorbed water in front of the drop plays its part in making the spreading a very slow process.

4. Summary

The wetting behavior of (relatively) dilute aqueous surfactant solutions over highly hydrophobic and moderately hydrophobic polymer surfaces was characterized by wetting dynamics measurements. In order to analyze the equilibrium state, an algorithm to correct the contact angle taking evaporation into account is presented.

Considering the dynamic wetting behavior, it was found that ionic surfactant solutions such as SDS and DTAB do not spread on low energy surfaces ($\leqslant 23\ \mathrm{mJ/m^2}$) at any concentrations and they do spread over moderately hydrophobic surfaces (with surface energy about $36\ \mathrm{mJ/m^2}$). Admittedly, the cationic DTAB began to spread at the concentration of $(1/4)$cmc, whereas for anionic SDS the spreading within the whole concentration region investigated is characteristic.

As to the nonionic $C_{12}E_5$, the wetting behavior of its aqueous solutions is quite different. This surfactant was found to enhance spreading in aqueous solutions on both highly hydrophobic and moderately hydrophobic surfaces, demonstrating rather universal behavior.

Considering the spreading velocity, we emphasize rather unusual dynamic wetting behavior, which is shown in the long-time regime. Such slow spreading process may be affected by low surrounding humidity and explained as a transfer of surfactant molecules on the bare hydrophobic surfaces in front of the moving liquid on the three-phase contact line according to Starov and co-workers.

Acknowledgments

This research is supported by Sasol Germany GmbH. Two of the authors (K.S. and V.R.) acknowledge the Saxon Ministry of Science and Art (SMWK, Germany) for financial support. We are grateful to Zoltán Mészáros from Repallon GmbH (Switzerland) for giving much useful advice on the wetting measurements using the FibroDAT tester, as well as to Nicole Petong and to Mikhail Motornov, both from the Institute of Polymer Research Dresden, for performing the AFM experiments and ellipsometric measurements, respectively.

References

[1] T. Stoebe, Z. Lin, R.M. Hill, M.D. Ward, H.T. Davis, Langmuir 13 (1997) 7270–7275.
[2] F. Tiberg, A.-M. Cazabat, Langmuir 10 (1994) 2301–2306.
[3] D.M. Eckmann, D.P. Cavanagh, A.B. Branger, J. Colloid Interface Sci. 242 (2001) 386–394.
[4] B. Frank, S. Garoff, Langmuir 11 (1995) 87–93.
[5] M. von Bahr, F. Tiberg, B.V. Zhmud, Langmuir 15 (1999) 7069–7075.
[6] T. Stoebe, R.M. Hill, M.D. Ward, H.T. Davis, Langmuir 13 (1997) 7276–7281.
[7] M. Cachile, A.M. Cazabat, Langmuir 15 (1999) 1515–1521.
[8] J.F. Joanny, J. Colloid Interface Sci. 128 (2) (1989) 407–415.
[9] J.B. Grotberg, D.P. Gaver, J. Colloid Interface Sci. 178 (1996) 377–378.
[10] M. von Bahr, F. Tiberg, V. Yaminsky, Colloids Surf. A 193 (2001) 85–96.
[11] F. Tiberg, B. Zhmud, K. Hallstensson, M. von Bahr, Phys. Chem. Chem. Phys. 2 (2000) 5189–5196.
[12] N. Mourougou-Candoni, B. Prunet-Foch, F. Legay, M. Vignes-Adler, K. Wong, J. Colloid Interface Sci. 192 (1997) 129–141.
[13] Z. Király, G.H. Findenegg, J. Phys. Chem. B 102 (1998) 1203–1211.
[14] D.Y. Kwok, A.W. Neumann, Adv. Colloid Interface Sci. 81 (1999) 167–249.
[15] S. Gerdes, G. Ström, Colloids Surf. 116 (1996) 135–144.
[16] S.M. Rowan, M.L. Newton, G. McHale, J. Phys. Chem. 99 (1995) 13,268–13,271.
[17] V.M. Starov, personal communication.
[18] V.M. Starov, S.R. Kosvintsev, M.G. Velarde, J. Colloid Interface Sci. 227 (2000) 185–190.
[19] E. Wolfram, É. Boross-Vargha, Fortschr. Kolloid. Polym. 55 (1971) 143–148.